Journal of Applied Sciences

ISSN 1812-5654

science alert

ANSInet
an open access publisher
http://ansinet.com

Journal of Applied Sciences 9 (2): 327-333, 2009
ISSN 1812-5654
© 2009 Asian Network for Scientific Information

Irreversibilities in Duct Geometries of Rhombic and Circular with Constant Wall Heat Flux and Laminar Flow

[1]H. Taherian and [2]H. Mirgolbabaei
[1]Department of Mechanical Engineering, Babol Noshirvani University of Technology, P.O. Box 484, Babol, Iran
[2]Department of Mechanical Engineering, KN Toosi University of Technology, Mollasadra, Tehran, Iran

Abstract: In this study, a second law comparison of irreversibility is used to determine the optimum duct geometry which minimizes losses for a range of laminar flows with constant wall heat flux condition. Water as a working fluid is considered. The duct geometries used are rhombic with various angle of bevel and circular. Hydraulic diameters are used for the different geometries. The rhombic geometry with the angle of 90°, when the frictional contributions of entropy generation become important is the best. Also power required to overcome fluid friction in the mentioned duct is smallest.

Key words: Irreversibilities, laminar flow, constant wall heat flux, convection, rhombic

INTRODUCTION

The optimal design criteria for thermal systems can be achieved by minimizing entropy generation in the systems. This problem has been the topic of great interest in fields such as heat exchangers, energy-storage systems, power plants, refrigeration and space applications. There may exist an optimal thermodynamic design of these systems which minimizes the amount of entropy generation. Increased effort is being directed at producing more efficient heat exchangers to affect savings of energy, material and labor. Improvements in heat-transfer augmentation depend on performance and manufacturing cost (Kakac *et al*., 1981). Consequently, there is increased need for utilization of a variety of duct geometries for heat-transfer applications with forced convection and internal flow. Ko and Ting (2006a) analyzed entropy generation induced by forced convection in a curved rectangular duct with external heating by numerical methods. The problem is assumed as steady, three-dimensional and laminar. They analyzed the local entropy generation distributions as well as the overall entropy generation in the whole flow fields, including the entrance region and fully developed region. Ko (2006) analyzed the optimal mass flow rate for steady, laminar, fully developed, forced convection in a helical coiled tube with fixed size and constant wall heat flux by the thermodynamic second law based on the minimal entropy generation principle. Two working fluids, namely air and water, were considered. Ko and Ting (2006b) analyzed the optimal Reynolds for the steady, laminar, fully developed forced convection in a helical coiled tube with constant wall heat flux based on minimal entropy generation principle. Two working fluids, water and air, were considered. It is found that the entropy generation distributions are relatively insensitive to coil pitch. Also they proposed a correlation equation for the optimal Reynolds as a function of curvature ratio and two dimensionless duty parameters, after a least-square-error analysis. Ko (2006) analyzed the optimal curvature ratio for steady, laminar, fully developed forced convection in a helical coiled tube with constant wall heat flux. Also he proposed a correlation equation for the optimal curvature ratio as a function of Reynolds and two dimensionless duty parameters through a least-square-error analysis. Different criteria for selecting and optimizing the heat-exchanger passage geometries were outlined by Bergles (1997). Because of size and volume constraints in applications to aerospace, nuclear, biomedical engineering and electronics, it may be required to use non-circular flow-passage geometries, particularly in compact heat exchangers and solar collectors. Analytical solutions of heat transfer and pressure drop for laminar flows in many duct geometries are available in the literature (Shah, 1975). In order to enhance the heat transfer, longitudinal fins and twisted tapes are being used in circular and noncircular ducts. Heat transfer enhancement is achieved at the expense of pumping power due to the increased friction factor. Efficient utilization of exergy has become one of the primary objectives in designing any thermodynamic system. Minimization of entropy generation in thermodynamic systems leads to efficient use of exergy

Corresponding Author: Hessam Mirgolbabaei, No. 40, Tohid 26, Janbazan blvd, Postal Code 4718767863, Babol, Iran
Tel: +989111139195

(Bejan, 1996). The irreversibilities associated with fluid flows through ducts are usually related to heat transfer and viscous friction. Different mechanisms and design features contributing to irreversibilities often compete with one another (Bejan, 2006). Therefore, there may exist an optimal thermodynamic design which minimizes entropy generation. Irreversibilities in various duct geometries with constant wall heat flux and laminar flow were studied by Sahin (1998). Correlations of optimal body sizes with external forced-convection heat transfer were discussed by Fowler and Bejan (1994). Bejan (1980, 1982) presented the procedure for entropy-generation minimization at the system-component level. Nag and Kumar (1989) studied second law optimization for convective heat transfer through a duct with constant heat flux and plotted the variation of entropy generation vs. the temperature difference between the bulk flow and surface using a duty parameter. For this case (Nag and Kumar, 1989), the product of Stanton number and temperature difference between the bulk and surface is constant owing to the constant heat flux imposed on the surface. Laminar heat convection in ducts of irregular cross sections was studied by Uzun and Unsal (1997). They analyzed forced convective heat transfer during hydrodynamic fully developed laminar fluid flow inside ducts of irregular cross section utilizing numerical methods.

Here, we discuss various duct geometries. The entropy generation and pumping power required are compared in order to find the optimum duct geometry which minimizes exergetic losses for a range of laminar flows and specified wall heat flux. Rhombic cross-section risers are being used by some manufactures of solar flat-plate collectors. It is customary in design to treat those cross sections as similar to circular tubes only using an equivalent hydraulic diameter. Due to difference in geometry between the two cross-sections i.e., circular and rhombic it is reasonable to doubt their exactly similar thermal and hydraulic behaviors. The present study is intended to shed some light on this matter.

Entropy generation and required pumping power analysis: In order to calculate the entropy generation, we consider an axially uniform duct of arbitrary cross section with a specified heat flux imposed on its surface. An incompressible viscous fluid with mass flow rate $\dot{m} = \rho \bar{U} A_C$ and inlet temperature T_O enters the duct of length L. Heat transfer to the bulk of the fluid occurs through the heat transfer coefficient h, which is taken as constant along the surface of the duct for fully developed laminar flow and constant thermophysical properties.

The entropy generation within a control volume of thickness dx along the duct is (Bejan, 2006):

$$d\dot{S}_{gen} = \dot{m} ds - \delta\dot{Q} / T_W \quad (1)$$

For an incompressible fluid

$$ds = C_P dT / T - dP / (\rho T) \quad (2)$$

and

$$\delta\dot{Q} = \dot{m} C_P dT = q'' p dx, \quad (3)$$

where, p is the perimeter of the duct. Integrating Eq. 3, the bulk temperature variation of the fluid and the total heat transfer along the duct are:

$$T = T_o + (4q'' / \rho \bar{U} D_H C_P) x \quad (4)$$

and

$$\dot{Q} = q'' pL \quad (5)$$

respectively. The pressure drop in Eq. 2 is (Kreith and Bohn, 1993):

$$dP = -(f \rho \bar{U}^2 / 2D_H) dx \quad (6)$$

where, f is the friction factor. A dimensionless total entropy generation based on the flow stream heat capacity rate $(\dot{m} C_P)$ is defined as (Sahin, 1998):

$$\psi = \dot{S}_{gen} / \dot{m} C_P = \dot{S}_{gen} / (\dot{Q} / \Delta T) \quad (7)$$

where, ΔT is the increase of the fluid temperature, $T_{(x=L)} - T_o$ (Sahin, 1996). Integrating Eq. 1 along the duct length L and by using Eq. 2-6, the dimensionless total entropy generation becomes:

$$\psi = \ln[(1 + 4St\tau\lambda)(1 + \tau) / (1 + \tau + 4St\tau\lambda)] + fEc / (8St) \ln(1 + 4St\tau\lambda) \quad (8)$$

where, $\tau = (T_W - T) / T_O = (q'' / h) / T_O, \lambda = L / D_H$ the Stanton number is $St = h / \rho \bar{U} C_P = Nu / RePr$ and the Eckert number is:

$$Ec = \bar{U}^2 / [C_P (T_W - T)] = \bar{U}^2 / [C_P (q'' / h)]$$

Equation 8 may be written as:

$$\psi = \ln[(Re + \tau\Pi_1)(1 + \tau) / (Re + \tau Re + \tau\Pi_1)] + \Pi_2 Re^2 \ln[(Re + \tau\Pi_1) / Re] \quad (9)$$

Therefore

$$\psi = \psi_T + \psi_P \quad (10)$$

Table 1: Hydraulic diameters of the ducts used

Duct geometry	Hydraulic diameter (D_H)
Circular	$\frac{2}{\sqrt{\pi}}\sqrt{A_C}$
Rhombic	$\sqrt{A_C}\sqrt{\sin\theta}$

Where:

$$\psi_T = \ln[(Re+\tau\Pi_1)(1+\tau)/(Re+\tau Re+\tau\Pi_1)] \quad (11)$$

$$\psi_P = \Pi_2 Re^2 \ln[(Re+\tau\Pi_1)/Re] \quad (12)$$

and also $\Pi_1 = 4Nu\lambda/Pr$ and $\Pi_2 = \mu^3(fRe)/8\rho^2 D_H^3 q''$.

Ψ_T and Ψ_P represent the contribution of entropy generation from heat transfer irreversibility and fluid friction irreversibility, respectively.

For a given duct geometry and a stream with constant properties, the dimensionless numbers Π_1 and Π_2 are constant. Therefore, Ψ is a function of Re and τ only. Values of Nu and f Re for fully developed laminar flow are given by Shah (1975) for a variety of duct geometries. The hydraulic diameter may be calculated from $D_H = 4A_C/P$ for all geometries (Table 1).

A modified dimensionless entropy generation may be based on the total rate of heat transfer, viz.,

$$\phi = (q''/h)\dot{S}_{gen}/\dot{Q} \quad (13)$$

Where:

$$\phi = (Re/\Pi_1)\psi \quad (14)$$

The power required to overcome fluid friction in the duct is related to the total heat transfer rate by:

$$P_r = A_C \Delta P \bar{U}/\dot{Q} \quad (15)$$

where, ΔP is the total pressure drop in the duct. From Eq. 5 and 6, the pumping power to heat transfer rate ratio for fully developed laminar flow becomes:

$$P_r = \Pi_2 Re^2 \quad (16)$$

DISCUSSION

Water has been used as working fluid. The thermophysical parameters used are shown in Table 2.

In order to understand the detailed contribution of entropy generation from frictional irreversibility and heat transfer irreversibility, investigations of the effects of Re on Ψ_P and Ψ_T have been carried out for duct with circular cross-section in Fig. 1. The competition between the entropy generation from frictional irreversibility and heat transfer irreversibility can be seen very different in various Re numbers.

Table 2: Thermophysical properties of water and the parameters used

Parameter	Numerical value
A_C (m^2)	(2 to 8) 10^{-6} and 6.34×10^{-5}
C_P (J kg^{-1} K^{-1})	4282
L (m)	1.0
Pr	7
q'' (W m^{-2})	250 to 1000
T_O (K)	292
μ (Ns^{-1} m^{-2})	9.93×10^{-4}
ρ (kg m^{-3})	998.2

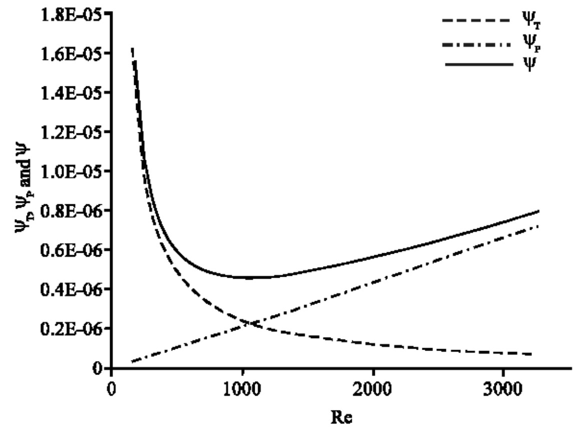

Fig. 1: The influence of Re on Ψ_P and Ψ_T of a baseline case (circular) with $A_C = 4\times10^{-6}$ m^2 and q'' = 500 W m^{-2}

As can be seen, the value of Ψ_P is nearly zero for low Re, which indicates the major entropy generation comes from heat transfer irreversibility. As Reynolds increased, it can be seen that Ψ_P increases but Ψ_T decreases. However, Ψ_T is still much larger than Ψ_P, which implies the entropy generation is dominated by the heat transfer irreversibility for low Reynolds numbers. When Re further increases to 1050, the curves of Ψ_P and Ψ_T intersect. When Re is larger than the intersection Re, Ψ_P is larger than Ψ_T and vice verse. It indicates the entropy generation due to frictional irreversibility becomes the dominant source.

Since heat transfer irreversibility dominates in lower Re region, the change of Ψ_T is more appreciable in lower Re cases. For the similar reason, the changes of Ψ_P are more appreciable in larger Re cases since frictional irreversibility dominates in larger Re region.

Such influences of Re on entropy generation could be understood from the effects of Re on fluid friction and heat transfer performance. As Re increases, the fluid

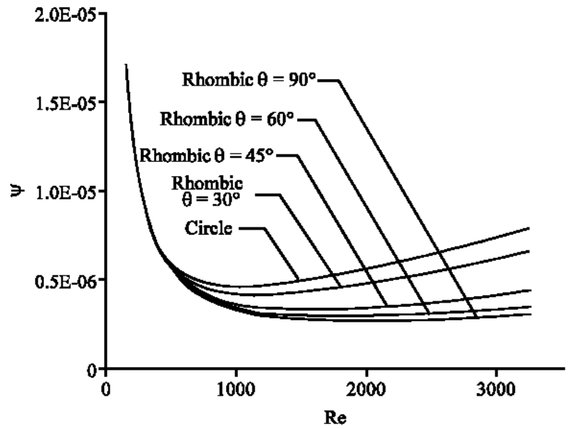

Fig. 2: Dimensionless entropy generation Ψ versus Re for various duct geometries; A_C = 4×10^{-6} m^2 and q" = 500 W m^{-2}

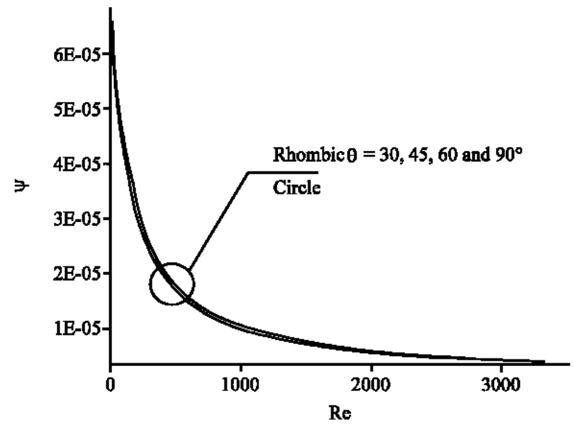

Fig. 3: Dimensionless entropy generation Ψ versus Re for various duct geometries; A_C = 6.34×10^{-5} m^2 and q" = 500 W m^{-2}

friction in flow fields will increase and thus results in the increase of entropy generation due to friction irreversibility.

On the contrary, the increase of Re will enhance the heat transfer performance, making the temperature gradient in flow fields become gentle and in turn results in the decrease of heat transfer irreversibility and entropy generation.

Figure 2 shows the variation of Ψ with Re for the five selected duct geometries. The cross section A and T_O were constant.

As can be shown, in the lower Reynolds region, with increase of Re, the entropy generation will decrease and in the larger Reynolds region, with increase of Re, the entropy generation will increase.

Ψ includes terms from heat transfer and viscous friction. Since the entropy generation in the lower Reynolds cases is dominated by heat transfer irreversibility, the change of Ψ is mainly determined by Ψ_T. As discussed previously, the increase of Re would enhance heat transfer performance and in turn reduce the heat transfer irreversibility, therefore, Ψ in these cases can be seen to decrease monotonically with increase of Re.

As Reynolds further increases, in the larger Re, the entropy generation takes a totally different trend, while with the increase of Reynolds, the entropy generation increases. Such results come from that, for larger Reynolds, the frictional irreversibility becomes dominant as Re increases and the more serious entropy generation due to frictional irreversibility would be raised when Re increases. Although the heat transfer irreversibility would decrease simultaneously, its contribution is relatively minor in these cases and therefore the resultant entropy generation is determined by frictional irreversibility.

As can be shown, the rhombic geometry with θ = 90, gives the lowest dimensionless entropy generation and circle geometry has a largest dimensionless entropy generation.

As Re increases, the effect of geometry disappears and the dimensionless entropy generation becomes a function of (τ), i.e.,

$$\lim_{Re\to 0} \psi = \ln(1+t) \qquad (17)$$

Also, as $A_c \to \infty$ the effect of geometry disappears and the dimensionless entropy generation becomes the same function mentioned above. To clarify this, Fig. 3 shows the variation of Ψ with Re for the five selected duct geometries for A_C = 6.34e−5.

Comparison of duct geometries using ϕ may be appropriate when the total heat transfer rate is important as shown in Fig. 4.

As Re is increased, the entropy generation will increase. In the Reynolds greater than 550, the value of ϕ will be decreased with the increase of θ, such that for the range of laminar flow, this trend will be prevailed.

The pumping power required to overcome viscous friction is shown in Fig. 5. The rhombic geometry with ϕ = 90° is superior to all other geometries.

Figure 6-8 show the effect of cross section A_C on Ψ, ϕ and P_r, respectively. The rhombic geometry with ϕ = 90° has been selected as a representative case. The minima that exist for Ψ are functions of Re as shown in Fig. 6. Therefore, minimum entropy generation for laminar flows may not exist for all geometries. Both entropy generation and pumping power generally increase as the cross section area is decreased.

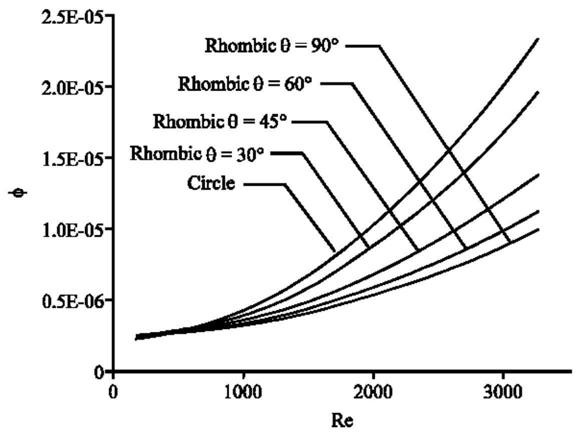

Fig. 4: Modified dimensionless entropy generation Ψ versus RE for various duct geometries; $A_C = 4\times10^{-6}$ m^2 and q" = 500 W m^{-2}

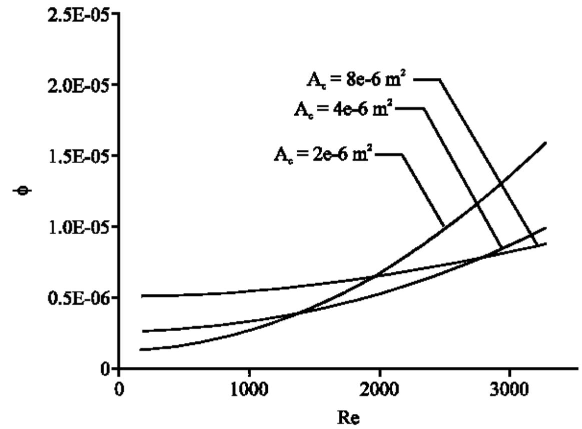

Fig. 7: Modified dimensionless entropy generation versus φ Re for rhombic geometry with of different cross sectional area; q" = 500 W m^{-2}

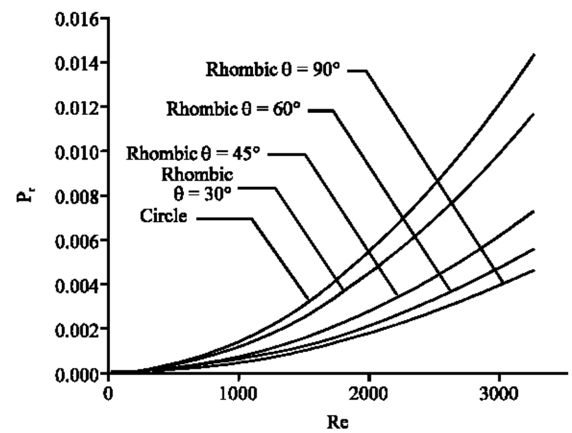

Fig. 5: Pumping power to heat transfer ratio P_r versus Re for various duct geometries; $A_C = 4\times10^{-6}$ m^2 and q" = 500 W m^{-2}

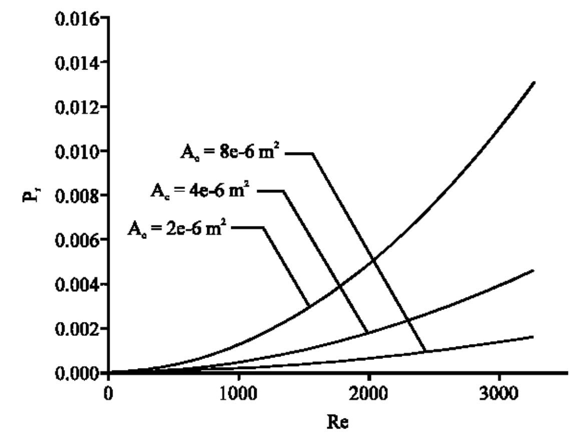

Fig. 8: Pumping power to heat transfer ratio P_r versus Re for rhombic geometry with φ = 90° of different cross sectional area; q" = 500 W m^{-2}

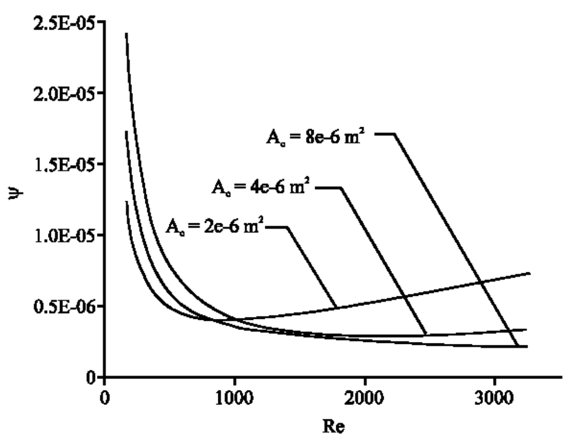

Fig. 6: Dimensionless entropy generation Ψ versus Re for rhombic geometry with φ = 90° of different cross sectional area; q" = 500 W m^{-2}

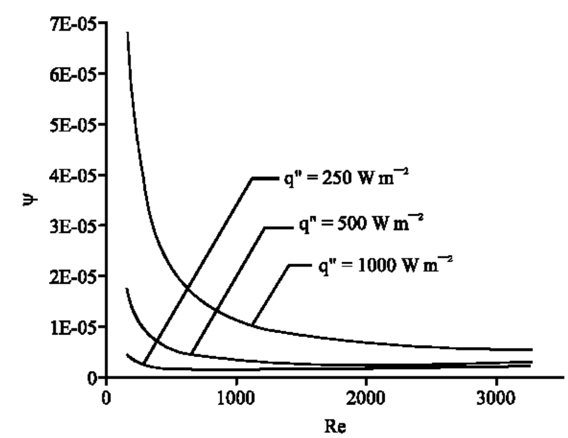

Fig. 9: Dimensionless entropy generation Ψ versus Re for rhombic geometry with φ = 90° with different wall heat fluxes; $A_C = 4\times10^{-6}$ m^2

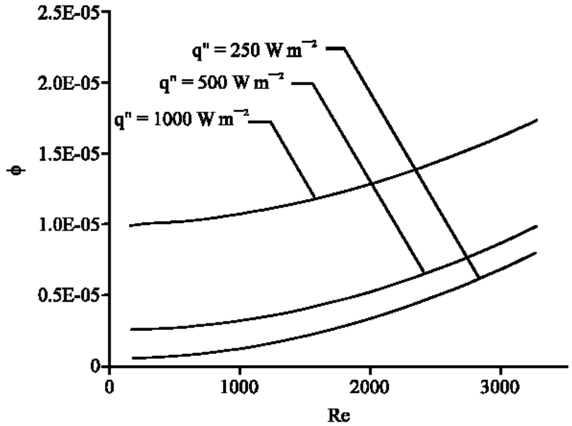

Fig. 10: Modified dimensionless entropy generation ϕ versus Re for rhombic geometry with ϕ = 90° with different wall heat fluxes; $A_C = 4\times10^{-6}$ m^2

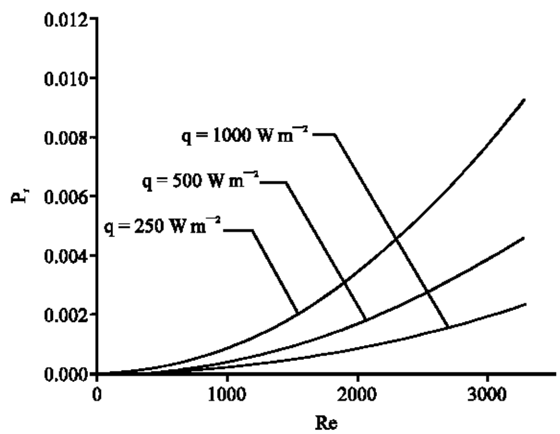

Fig. 11: Pumping power to heat transfer ratio P_r versus Re for rhombic geometry with ϕ = 90° with different wall heat fluxes; $A_C = 4\times10^{-6}$ m^2

Figure 9-11 show the effects of wall heat flux on Ψ, ϕ and P_r, respectively. Both entropy generation and pumping power are influenced by wall heat flux. As the heat flux is increased, the entropy generation increases but the pumping power per unit heat transfer rate decreases. In the limit when $\tau \to 0$, the entropy generation becomes a linear function of Re, viz.,

$$\lim_{\tau\to 0}\psi = [(f\,Re)\mu^2 L/2\rho^2 D_H^3 C_P T_O]Re \qquad (18)$$

CONCLUSION

A numerical investigation of entropy generation in ducts of rhombic cross section has been performed and the results compared to circular tube. It was found that the rhombic duct performs better than the circular duct and among ducts of various side angles the one with a 90° angle can be considered the best. The effect of area cross section and the value of heat flux were also investigated. Increasing cross sectional area increased entropy generation. The same was found to be true for increased heat flux. In some cases there seemed to exist minimum value of entropy generation at a certain Re.

NOMENCLATURE

A_C = Flow cross sectional area (m^2)
C_P = Specific heat capacity (J kg^{-1} K^{-1})
D_H = Hydraulic diameter (m)
E_c = Eckert No. $[\bar{U}^2/[C_P(q''/h)]$
f = Friction factor
h = Heat transfer coefficient (W m^{-2} K^{-1})
k = Thermal conductivity (W m^{-1} K^{-1})
L = Length of the duct (m)
$\dot{m}$ = Mass flow rate (kg sec^{-1})
Nu = Nusselt No. (hD_H/k)
p = Perimeter (m)
P = Pressure (N m^{-2})
P_r = Pumping power to heat transfer ratio $(A_C\Delta P\bar{U}/\dot{Q})$
Pr = Prandtl No. ($\mu C_P/k$)
q" = Wall heat flux (W m^{-2})
$\dot{Q}$ = Total heat transfer (W)
Re = Reynolds No. $(\rho\bar{U}D_H/\mu)$
S = Entropy (J kg^{-1} K^{-1})
$\dot{S}_{gen}$ = Entropy generation (W K^{-1})
St = Stanton No. $(h/(\rho\bar{U}C_P))$
T = Temperature (K)
T_O = Inlet temperature (K)
T_W = Wall temperature (K)
U = Fluid bulk velocity (m sec^{-1})
x = Axial distance (m)
ΔP = Total pressure drop (N m^{-2})
ΔT = Increase of fluid bulk temperature (K)
μ = Viscosity (Ns^{-1} m^{-2})
λ = Dimensionless axial distance (L/D_H)
Π_1 = Dimensionless group ($4Nu\lambda/Pr$)
Π_2 = Dimensionless group $(\mu^3(fRe)/8\rho^2 D_H^3 q'')$
ϕ = Modified dimensionless entropy generation $((q''/h)\dot{S}_{gen}/\dot{Q})$
Ψ = Dimensionless entropy generation $(\dot{S}_{gen}/(\dot{Q}/\Delta T))$
Ψ_T = Contribution of entropy generation from heat transfer irreversibility
Ψ_P = Contribution of entropy generation from fluid friction irreversibility
ρ = Density (kg m^{-3})
τ = Dimensionless wall heat flux $((q''/h)/T_O)$

REFERENCES

Bejan, A., 1980. Second law analysis in heat transfer. Energy, 5: 720-732.

Bejan, A., 1982. Second-Law analysis in heat transfer and thermal design. J. Adv. Heat Transfer, 15: 1-58.

Bejan, A., 1996. Entropy Generation Minimization: The Method of Thermodynamic Optimization of Finite-Size Systems and Finite-Time Processes. 1st Edn., CRC Press, Boca Raton, Florida, ISBN: 9780849396519.

Bejan, A., 2006. Advanced Engineering Thermodynamics. 1st Edn., John Wiley and Sons, New York, ISBN: 978-0-471-67763-5.

Bergles, A.E., 1997. Heat transfer enhancement: The encouragement and accommodation of high heat fluxes. J. Heat Transfer, 119: 8-19.

Fowler, A.J. and A. Bejan, 1994. Correlation of optimal sizes of bodies with external forced convection heat transfer. Int. Comm. Heat Mass Transfer, 21: 17-27.

Kakac, S., A.E. Bergles and F. Mayinger, 1981. Heat Exchangers Thermal-Hydraulic Fundamentals and Design. 1st Edn., Hemisphere Publishing Corporation, Washington, New York, London, ISBN: 0070332843.

Ko, T.H., 2006. Thermodynamic analysis of optimal mass flow rate for fully developed laminar forced convection in a helical coiled tube based on minimal entropy generation principle. Energy Conv. Manage., 47: 3094-3104.

Ko, T.H. and K. Ting, 2006a. Entropy generation and optimal analysis for laminar forced convection in curved rectangular ducts: A numerical study. Int. J. Thermal Sci., 45: 138-150.

Ko, T.H. and K. Ting, 2006b. Optimal Reynolds number for the fully developed laminar forced convection in a helical coiled tube. Energy, 31: 2142-2152.

Kreith, F. and M.S. Bohn, 1993. Principles of Heat Transfer. 5th Edn., West Publications, New York, ISBN-13: 9780700224227.

Nag, P.K. and N. Kumar, 1989. Second law optimization of convective heat transfer through a duct with constant heat flux. Int. J. Energy Res., 13: 537-543.

Sahin, A.Z., 1996. Thermodynamics of laminar viscous flow through a duct subjected to constant heat flux. Energy, 21: 1179-1187.

Sahin, A.Z., 1998. Irreversibilities in various duct geometries with constant heat flux and laminar flow. Energy, 23: 465-473.

Shah, R.K., 1975. Laminar flow friction and forced convection heat transfer in ducts of arbitrary geometry. Int. J. Heat Mass Transfer, 18: 849-862.

Uzun, I. and M. Unsal, 1997. A numerical study of laminar heat convection in ducts of irregular cross section. Int. Comm. Heat Mass Transfer, 24: 835-848.